 DOI: 10.1002/maco.201106321

Effect of thermal oxidation on the corrosion resistance of Ti6Al4V alloy in hydrochloric and nitric acid medium

M. Jamesh, Satendra Kumar, T. S. N. Sankara Narayanan* and P. K. Chu

The characteristics of Ti6Al4V alloy subjected to thermal oxidation in air atmosphere at 650 °C for 48 h and its corrosion behavior in 0.1 and 4 M HCl and HNO_3 medium are addressed. When compared to the naturally formed oxide layer (~4–6 nm), a relatively thicker oxide scale (~7 μm) is formed throughout the surface of Ti6Al4V alloy after thermal oxidation. XRD pattern disclose the formation of the rutile and oxygen-diffused titanium as the predominant phases. A significant improvement in the hardness (from 324 ± 8 to 985 ± 40 $HV_{0.25}$) is observed due to the formation of hard oxide layer on the surface followed by the presence of an oxygen diffusion zone beneath it. Electrochemical studies reveal that the thermally oxidized Ti6Al4V alloy offers a better corrosion resistance than its untreated counterpart in both HCl and HNO_3 medium. The uniform surface coverage, compactness and thickness of the oxide layer provide an effective barrier towards corrosion of the Ti6Al4V alloy. The study concludes that thermal oxidation is an effective approach to engineer the surface of Ti6Al4V alloy to increase its corrosion resistance in HCl and HNO_3 medium.

1 Introduction

Titanium and its alloys have become the materials of choice in many industries due to their excellent corrosion resistance in a wide variety of environments [1]. The formation of a thin self-adherent passive oxide film on their surfaces is considered responsible for this attribute. The corrosion rate of titanium and its alloys, however, is significant in hydrofluoric acid, caustic solutions, and uninhibited concentrated hydrochloric or sulfuric acid solutions that dissolve the protective oxide film or limit its formation. The increased use of titanium and its alloys in extractive metallurgy has prompted research on their corrosion behavior in various acids [2–6]. Since the passive film is responsible for the excellent corrosion resistance of titanium and its alloys, it is obvious that any treatment or modification that facilitates its formation and thickening would offer improved corrosion performance. Addition of strongly oxidizing inorganic compounds such as $K_2Cr_2O_7$, $KMnO_4$, KIO_3, Na_2MoO_4, $NaClO_3$, Cl_2, and H_2O_2 tend to promote passivation of titanium. Addition of anions such as iodate (IO_3^-), metavanadate (VO_3^-) and molybdate (MoO_4^{2-}) promoted passivation of Ti-6Al-4V alloy in 2.5 M H_2SO_4, and 5.0 M HCl [2]. Alloying of titanium with molybdenum, chromium, aluminium, zirconium, tantalum, which increases its tendency to passivate, also enable a beneficial influence.

Surface modification is a promising approach to increase the surface hardness, corrosion resistance and wear resistance of titanium and its alloys. Numerous surface modification methods such as, chemical treatment (acid and alkali treatment), electrochemical treatment (anodic oxidation), chemical vapor deposition, physical vapor deposition, sol–gel coatings, plasma spray deposition, ion implantation, thermal oxidation, etc., have been explored [7–17]. Among them, thermal oxidation is considered as a cost-effective method to deliberately generate a barrier oxide layer of relatively higher thickness (~20–80 μm) on titanium compared to the naturally formed oxide layer (typically of 4–6 nm). Thermal oxidation of titanium is aimed to produce in situ ceramic coatings, mainly based on rutile, in the form of a thick, crystalline oxide film, which is accompanied by the dissolution of oxygen beneath them. The thermally formed oxide layer enables an increase in hardness; wear resistance and

M. Jamesh, P. K. Chu
Department of Physics and Material Science, City University of Hong Kong, Tat Chee Avenue, Kowloon (Hong Kong)

S. Kumar, T. S. N. Sankara Narayanan
CSIR-National Metallurgical Laboratory, Madras Centre, CSIR Madras Complex, Taramani, Chennai-600 113 (India)

T. S. N. Sankara Narayanan
Present address: Department of Dental Biomaterials and Institute of Oral Bioscience, School of Dentistry, Chonbuk National University, Jeonju 561-756, (South Korea)
E-mail: tsnsn@rediffmail.com

corrosion resistance of titanium and its alloys [8–16]. The ability of thermally oxidized (TO) commercially pure titanium (CP-Ti) and Ti6Al4V alloy in improving the corrosion and fretting corrosion resistance in Ringer's solution and also the effect of thermal oxidation on corrosion resistance of CP-Ti in hydrochloric and nitric acid medium were reported in our earlier papers [8–11]. The present paper aims to address the corrosion behavior of TO Ti6Al4V alloy in HCl and HNO_3 (0.1 and 4 M) medium evaluated by open circuit potential (OCP)–time measurement and potentiodynamic polarization studies.

2 Experimental details

The Ti6Al4V alloy (grade-5, chemical composition in wt%: N, 0.02; C, 0.03;H, 0.011; Fe, 0.22; O, 0.16; Al, 6.12; V, 3.93; and Ti: Balance) having a dimension of $3 \times 4 \times 0.2\,cm^3$ was used as the substrate material. Before thermal oxidation, the Ti6Al4V alloy samples were abraded using successive grit size of SiC-coated abrasive papers (60, 100, 220, 320, 400, 600, 800, and 1000 μm, respectively), followed by rinsing with deionized water and acetone. Thermal oxidation of Ti6Al4V alloy samples were performed using a muffle furnace in air atmosphere at 650 °C for 48 h. The samples were placed inside the furnace and, the temperature was increased at a constant heating rate of 5 °C/min. (the thermal treatment includes ramping step). Once it reached 650 °C, the samples were left at this temperature for 48 h (not including the ramp-up step). After thermal oxidation, the samples were allowed to cool in the furnace at its natural cooling rate. The phase constituents of untreated and TO Ti6Al4V alloy samples, and the nature of the oxide film formed on their surfaces were determined by X-ray diffraction (D8 DISCOVER, Brucker axs) using Cu-K_α radiation. The thickness of the oxide layer and the surface morphology of TO Ti6Al4V alloy were assessed by scanning electron microscope (SEM). The elemental composition on the surface of TO Ti6Al4V alloy was analyzed by energy dispersive X-ray (EDAX) analysis. The microhardness of untreated and TO Ti6Al4V alloy samples was measured using a Leica Vickers microhardness tester at a load of 0.25 N applied for 15 s. Seven indentations were made on each sample, and the values were averaged out. The corrosion behavior of untreated and TO Ti6Al4V alloy samples in HCl and HNO_3 medium (0.1 and 4 M) was evaluated by OCP–time measurements and potentiodynamic polarization studies using a potentiostat/galvanostat/frequency response analyzer of ACM instruments (Model: Gill AC). The untreated/TO Ti6Al4V alloy sample forms the working electrode, while a saturated calomel electrode (SCE) and graphite rod were used as the reference and auxiliary electrodes, respectively. These electrodes were placed within a flat cell in such a way that only $1\,cm^2$ area of the working electrode was exposed to the electrolyte solution. The HCl and HNO_3 (0.1 and 4 M) solutions were kept open to air and, maintained at 27 ± 1 °C. Before performing the potentiodynamic polarization studies, the untreated and TO Ti6Al4V alloy samples were allowed to stabilize in HCl and HNO_3 (0.1 and 4 M) for 30 min during which the change in OCP was recorded as a function of time. Potentiodynamic polarization measurements were carried out in the potential range from −250 to +3000 mV relative to OCP *versus* SCE at a scan rate of 1.67 mV/s. The very high potential (up to +3000 mV) is employed to study the passivation behavior. The corrosion potential (E_{corr}) and corrosion current density (i_{corr}) were determined from the polarization curves using Tafel extrapolation method. To compare the passivation ability, the passive current density (i_{pass}) of untreated and TO Ti6Al4V alloy, is determined at +900 mV *versus* SCE. Similar experimental conditions were also used in our earlier work [8–11, 18]. The potentiodynamic polarization studies were repeated at least three times to ensure reproducibility of the test results. Since the pattern/trend of the polarization curves do not exhibit any variation between the triplicate measurements, only one curve was selected as a representative curve for subsequent analysis.

3 Results and discussion

3.1 Characteristics of thermally oxidized Ti6Al4V alloy

The XRD patterns of untreated and TO Ti6Al4V alloy are shown in Fig. 1. Untreated Ti6Al4V alloy is comprised of α-Ti and α/β-Ti phases (denoted as "Ti"; and α/β-Ti in Fig. 1). The XRD pattern of TO Ti6Al4V alloy exhibits the presence of rutile (denoted as "R" in Fig. 1) and oxygen diffused Ti (denoted as "Ti(O)" in Fig. 1) as the predominant phases. Similar observations were also made earlier by other researchers [12, 15, 19, 20]. *Siva Rama Krishna* et al. [15] have reported the formation of TiO at temperatures <700 °C and rutile at 700 °C and above 800 °C, as dominant phases following oxidation of titanium. *Guleryuz* and *Cimenoglu* [19, 20] have reported the presence of anatase phase when Ti6Al4V alloy was oxidized at 600 °C for 24 and 48 h whereas rutile was the only dominated phase when the alloy was oxidized at 650 °C for 48 h. In this study, no anatase phase could be identified when the Ti6Al4V alloy samples are TO in air atmosphere at 650 °C for 48 h. The formation of oxygen diffusion layer on TO Ti and its alloys has also been confirmed by many researchers [21, 22]. Based on the elongation of "c" axis, increase

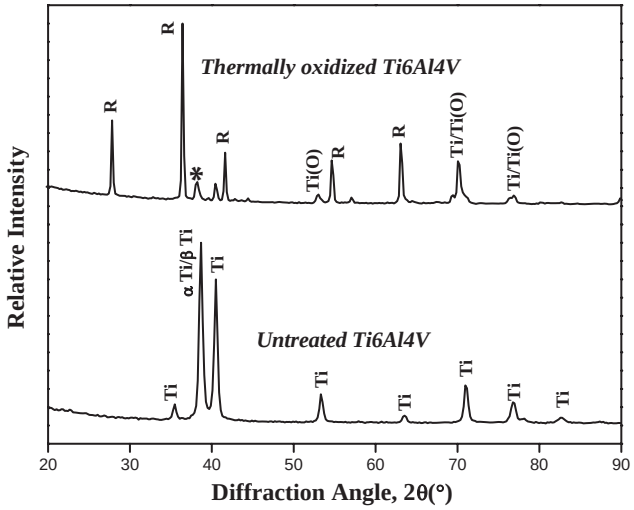

Figure 1. XRD patterns of untreated and TO (at 650 °C for 48 h in air atmosphere) Ti6Al4V alloy

in lattice parameter and increase in c/a ratio, *Yan* and *Wang* [21] have reported the formation of oxygen diffusion layer. *Ebrahimi* et al. [22] have confirmed the presence of dissolved oxygen in titanium, based on the broadening of the α-peaks and appearance of a shoulder pattern at lower diffraction angles. The X-ray diffraction pattern of Ti6Al4V alloy TO at 650 °C for 48 h in air atmosphere reveals a shift in peaks pertaining to α-Ti towards lower diffraction angles, suggesting an increase in lattice parameters. Broadening of the α-Ti peaks and appearance of a shoulder pattern (marked as * in Fig. 1) at lower diffraction angles confirm the presence of oxygen diffusion layers.

The cross-sectional view of the oxidized Ti6Al4V alloy sample (Fig. 2) clearly reveals the formation of oxide scales throughout the surface. The EDAX spectrum of the oxide layer formed on the surface of TO Ti6Al4V alloy oxidized at 650 °C for 48 h recorded in a particular region is shown in Fig. 3. The signals for Al, Ti, and O are observed whereas the signal for V is not observed. This suggests the presence of Al and Ti oxides in the oxide layer. However there is no aluminium oxides peak observed in the XRD. This observation shows that the presence of aluminium oxide concentration is very low when compared to the titanium oxide. *Garcia-Alonso* et al. [23] and *Du* et al. [24] had also observed the presence of aluminium oxides in the oxide layer of TO Ti6Al4V alloy.

The hardness profile of TO Ti6Al4V alloy measured as a function of distance from the surface is shown in Fig. 4. It is evident that thermal oxidation enabled a significant improvement in hardness of Ti6Al4V alloy. The hardness of the oxide layer at the surface is 985 ± 40 $HV_{0.25}$ and it remains constant for a few micrometer and then it decreased gradually until it reaches a stable value of 324 ± 8 $HV_{0.25}$ (similar to that of the untreated Ti6Al4V alloy) at a depth of 30 μm from the surface. The hardness

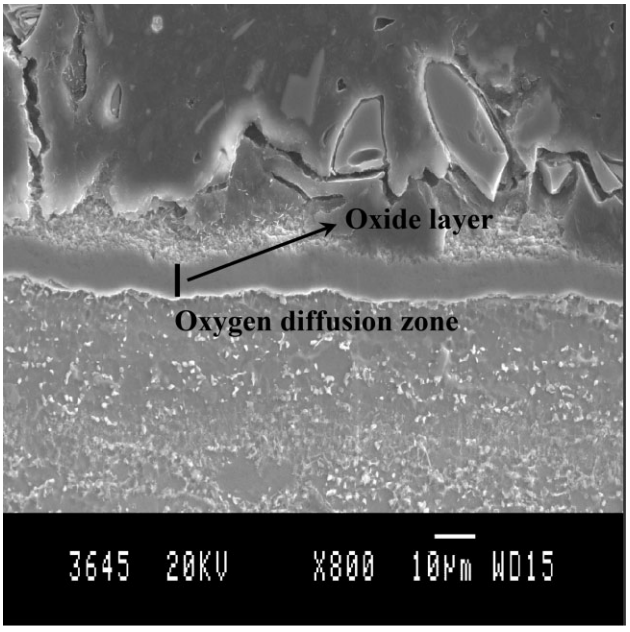

Figure 2. Scanning electron micrograph taken at the cross section of TO (at 650 °C for 48 h in air atmosphere) Ti6Al4V alloy

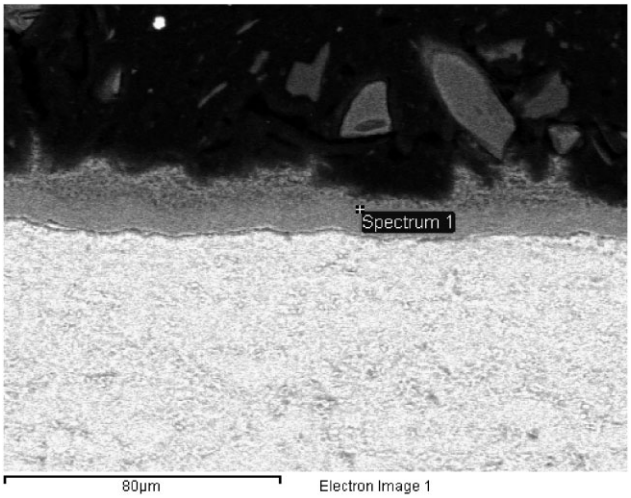

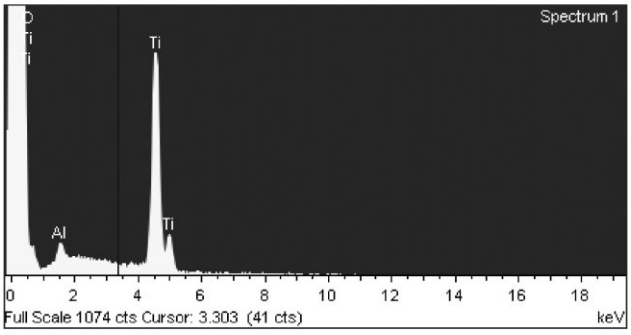

Figure 3. The selected area of the oxide layer used for the EDAX analysis and its corresponding EDX pattern of TO (at 650 °C for 48 h in air atmosphere) Ti6Al4V alloy

profile (Fig. 4) and cross sectional view (Fig. 2) confirm that the increase in hardness of TO Ti6Al4V alloy is due to the presence of hard oxide layer at the surface (~7 μm) followed by the presence of oxygen diffusion layer (~20 μm) beneath it.

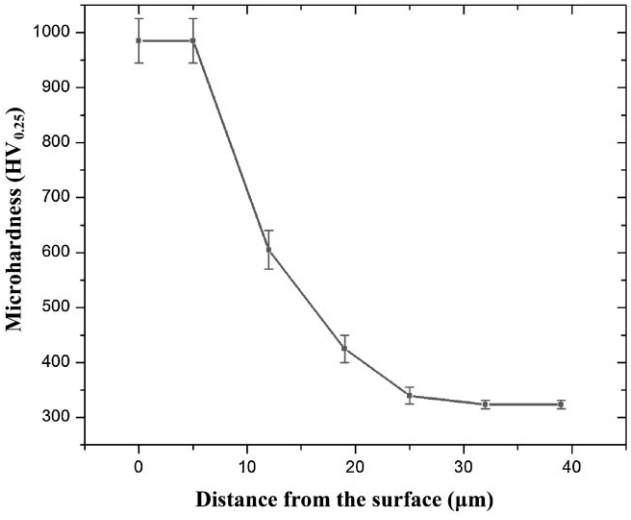

Figure 4. Hardness profile of Ti6Al4V alloy TO at 650 °C for 48 h in air atmosphere

It has been reported that the adhesion and mechanical properties of the oxide layer formed during thermal oxidation of Ti and its alloys are influenced by the experimental conditions used such as treatment temperature, time and air/furnace cooling [9, 15, 22, 25–27]. *Siva Rama Krishna* et al. [15] have observed a severe spallation and poor adhesion of the oxide layer when the oxidized samples were subjected to air-cooling. The fast cooling rate results in the generation of large thermal stresses due the high ratio of the coefficient of thermal expansion between the metal and oxide. In contrast, samples that were allowed to cool in the furnace exhibit very good adhesion with the substrate. According to them [15], oxide layers on CP-Ti prepared by thermal oxidation followed by furnace cooling possess low porosity, higher hardness with less deviation in hardness, good adhesive strength, and excellent friction characteristics and wear resistance than those subjected to air-cooling. *Leinenbach* and *Eifler* [27] have reported that thermal oxidation of CP-Ti at 570 °C for 3 h followed by air cooling (faster cooling rate) leads to a poor fatigue limit. According to them, the rate of cooling of the TO samples would significantly affect the mechanical properties of TO CP-Ti. If the oxide layer is compact with one narrow homogeneous diffusive zone and the oxygen content of the surface layer is increased, then an improvement in fatigue limit is expected. In contrast, compressive residual stress and crystalline nature of the oxide layer would decrease the fatigue limit [22, 25–27]. Hence, in the present study, the Ti6Al4V alloy samples were subjected to thermal oxidation at 650 °C for 48 h followed by furnace cooling at its natural cooling rate. The cooling rate is kept constant to avoid problems such as poor adhesion, spallation, and decrease in fatigue properties. This condition enables the formation of a uniform, compact and adherent oxide layer, free of cracks that possess a higher hardness.

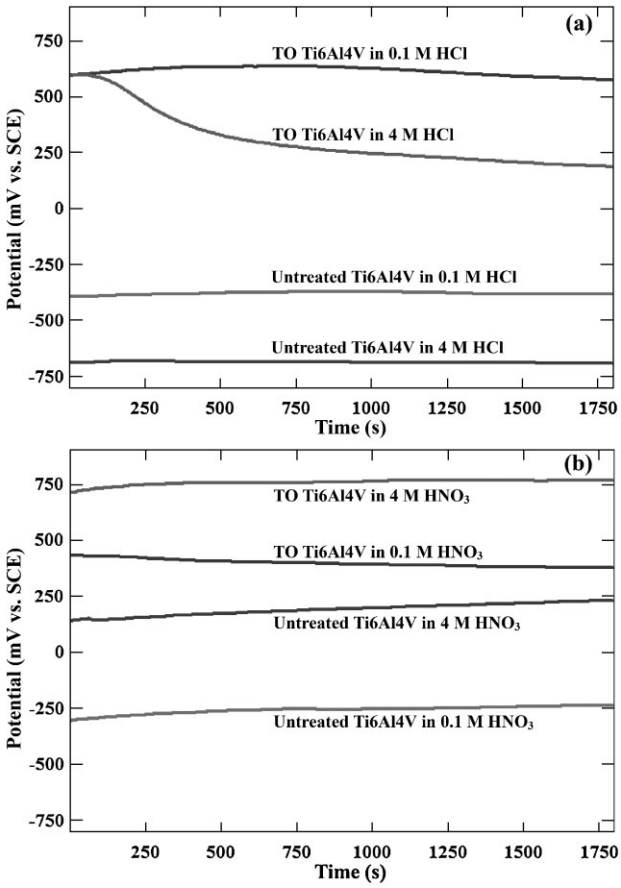

Figure 5. OCP–time curves of untreated and TO (at 650 °C for 48 h in air atmosphere) Ti6Al4V alloy in (a) HCl, and (b) HNO_3 medium

3.2 Corrosion behavior of untreated and thermally oxidized Ti6Al4V alloy

The OCP–time curves of untreated and TO Ti6Al4V alloy in HCl and HNO_3 medium (0.1 and 4 M) are shown in Fig. 5. TO Ti6Al4V alloy exhibits a nobler OCP in both HCl and HNO_3 medium when compared to its untreated counterpart. This indicates the ability of TO Ti6Al4V alloy to offer a better corrosion resistance in both HCl and HNO_3 medium [28].

A nobler shift in OCP is also observed with increase in concentration of HNO_3 from 0.1 to 4 M, for both untreated and TO Ti6Al4V alloy, which points out thickening of the passive film [29, 30]. This is due to the oxidizing nature of HNO_3, which promotes passivation and helps to increase the thickness of the passive layer. In contrast, increase in concentration of HCl from 0.1 to 4 M has resulted in a cathodic shift in OCP, which suggests dissolution of the oxide film.

The potentiodynamic polarization curves of untreated and TO Ti6Al4V alloy in HCl and HNO_3 medium are presented in Figs. 6a and b, respectively. Both untreated and TO Ti6Al4V alloy exhibit passivity in the anodic region of the polarization curves in both HCl and HNO_3 medium. In 0.1 M HCl and, 0.1 and 4 M HNO_3 medium, untreated Ti6Al4V alloy translates directly from ''Tafel region'' into a stable passive state, without exhibiting any active-passive transition whereas in 4 M HCl, it exhibits a stable passive state with an active-passive transition. However, TO Ti6Al4V alloy translates directly from the ''Tafel region'' into a passive state, without exhibiting any active-passive transition [31–33]. The passive current density (i_{pass}) is stable even up to +3000 mV *versus* SCE for TO Ti6Al4V alloy in both HCl and HNO_3 medium. The i_{pass} of TO Ti6Al4V alloy, measured at +900 mV *versus* SCE is relatively lower than that of its untreated counterpart. In general, materials that show a positive shift in corrosion potential (E_{corr}) and a decrease in i_{corr} would offer a better corrosion resistance and vice-versa [8–11, 16, 18]. The significant positive shift in E_{corr} and a substantial decrease in i_{corr} observed for TO Ti6Al4V alloy in both HCl and HNO_3 medium (0.1 and 4 M) clearly suggest its ability to offer a better corrosion resistance. The E_{corr}, i_{corr}, and i_{pass} of untreated and TO Ti6Al4V alloy are compiled in Table 1. Potentiodynamic polarization studies reveal that the TO Ti6Al4V offers a better corrosion resistance than the untreated Ti6Al4V in both HCl and HNO_3 medium (Fig. 6 and Table 1). The improvement in corrosion resistance is believed to be due to the coverage of its surface by relatively thicker oxide (~7 μm) scale when compared to the naturally formed oxide layer (~4–6 nm), which serves as an effective barrier layer, physically separating it from the acid medium. Since the oxide layer formed on the Ti6Al4V alloy is allowed to cool in the furnace than in air, it would possess a lower

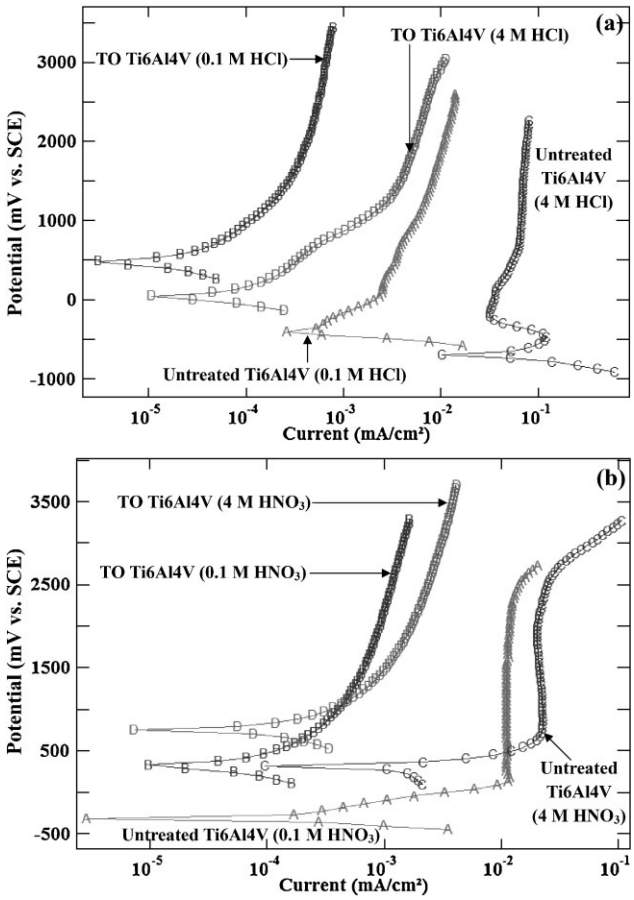

Figure 6. Potentiodynamic polarization curves of untreated and TO (at 650 °C for 48 h in air atmosphere) Ti6Al4V alloy in (a) HCl, and (b) HNO_3 medium

porosity [15]. If it was a porous layer, then it would not be possible to observe lower i_{corr} values from polarization studies. It has been reported in the literature that the experimental conditions used for thermal oxidation might result with either an effective barrier layer or porous layer [15, 22, 34]. Thermal oxidation on Ti and Ni–Ti alloys, and their characterization by impedance was studied by *Barisona* et al. [35]. The TO film on Ni–Ti alloy consists of outer porous layer due to the presence of Ni and inner compact layer having nickel free TiO_2 rutile. However, TO Ti sample consists of single compact layer. Several researchers have also confirmed the ability of TO CP-Ti and Ti6Al4V alloy to offer a better corrosion resistance in a variety of environments [8–11, 16, 19, 20]. *Guleryuz* and *Cimenoglu* [19] have reported that Ti6Al4V alloy subjected to thermal oxidation in air at 600 °C offered an excellent corrosion resistance than its untreated counterpart when they are subjected to accelerated corrosion test in 5 M HCl. According to those authors, no loss in weight is observed for TO Ti6Al4V alloy even after 36 h of immersion due to the formation of a thick and stable oxide film on the surface of the Ti6Al4V alloy. *Bloyce* et al. [16] have compared the corrosion resistance of untreated, plasma nitrided, TO and palladium-treated TO CP-Ti in 3.5% NaCl solution at room temperature by potentiodynamic polarization studies. Compared to untreated and plasma nitrided sample, TO samples exhibit a shift in E_{corr} towards the noble direction and a decrease in i_{corr}. Accelerated corrosion test in boiling 20% HCl reveals a several fold increase in lifetime for the TO CP-Ti samples compared to their untreated and plasma nitrided counterparts. The results of the present study further confirm the fact that thermal oxidation would lead to the formation of an effective barrier layer on Ti6Al4V alloy and would offer an excellent corrosion resistance compared to the untreated Ti6Al4V alloy in both HCl and HNO_3 medium at both 0.1 and 4 M concentrations.

4 Conclusions

Compared to the naturally formed oxide layer (~4–6 nm), thermal oxidation of Ti6Al4V alloy in air atmosphere at 650 °C for 48 h leads to the formation of a relatively thicker oxide scale (~7 μm) throughout the surface. Rutile and oxygen-diffused titanium have been observed as the predominant phases of the oxide layer, which enabled a significant improvement in the hardness 324 ± 8 to 985 ± 40 $HV_{0.25}$. TO Ti6Al4V alloy exhibits a nobler OCP in both HCl and HNO_3 medium when compared to its untreated counterpart. Increase in concentration of HNO_3 from 0.1 to 4 M leads to thickening of the passive film whereas a similar increase in concentration has resulted in thinning of the passive oxide film in HCl medium. The nobler E_{corr}, lower i_{corr}, and i_{pass} confirm the ability of TO Ti6Al4V alloy to offer a better corrosion resistance in both HCl and HNO_3 medium. The improvement in corrosion

Table 1. Corrosion potential (E_{corr}), corrosion current density (i_{corr}) and passive current density (i_{pass}) of untreated and TO Ti6Al4V alloy in HCl and HNO_3 medium calculated from potentiodynamic polarization studies

Type of sample tested	Electrolyte used	E_{corr} (mV vs. SCE)	i_{corr} (μA/cm^2)	i_{pass}^* (μA/cm^2)
Untreated Ti6Al4V alloy	0.1 M HCl	−407	1.1	3.4
	4 M HCl	−697	28.9	38.2
TO Ti6Al4V alloy	0.1 M HCl	+486	0.008	0.2
	4 M HCl	+45	0.03	1.2
Untreated Ti6Al4V alloy	0.1 M HNO_3	−317	0.2	11.2
	4 M HNO_3	+313	1.04	22.4
TO Ti6Al4V alloy	0.1 M HNO_3	+331	0.02	0.5
	4 M HNO_3	+748	0.07	1.1

*Measured at +900 mV vs. SCE.

resistance is due to the increase in thickness of the oxide layer (~7 μm) compared to the naturally formed one (~4–6 nm) that serves as an effective barrier layer, physically separating it from the acid medium. The study concludes that thermal oxidation is an effective means of engineering the surface to increase the corrosion resistance of the Ti6Al4V alloy in HCl and HNO_3 medium.

Acknowledgements: The authors express their sincere thanks to Dr. *S. Srikanth*, Director, National Metallurgical Laboratory, Jamshedpur and the Hong Kong Research Grants Council (RGC) General Research Funds (GRF) No. CityU 112510 to carry out this research work and permission to publish this paper.

5 References

[1] B. D. Craig, D. S. Anderson, *Handbook of Corrosion Data*, ASM International, Materials Park, OH **1995**.
[2] A. S. Mogoda, Y. H. Ahmad, W. A. Badawy, *Mater. Corros.* **2004**, *55*, 449.
[3] M. V. Popa, E. Vasilescu, P. Drob, C. Vasilescu, J. Mirza-Rosca, A. Santana Lopez, *Mater. Manuf. Process* **2005**, *20*, 35.
[4] J. Vaughan, A. Alfantazi, *J. Electrochem. Soc.* **2006**, *153*, B6.
[5] K. Azumi, M. Nakajima, K. Okamoto, M. Seo, *Corros. Sci.* **2007**, *49*, 469.
[6] R. Sh. Razavi, M. Salehi, M. Ramazani, H. C. Man, *Corros. Sci.* **2009**, *51*, 2324.
[7] X. Liu, P. K. Chu, C. Ding, *Mater. Sci. Eng. R* **2004**, *47*, 49.
[8] S. Kumar, T. S. N. Sankara Narayanan, S. Ganesh Sundara Raman, S. K. Seshadri, *Mater. Sci. Eng. C* **2009**, *29*, 1942.
[9] S. Kumar, T. S. N. Sankara Narayanan, S. Ganesh Sundara Raman, S. K. Seshadri, *Mater. Chem. Phys.* **2010**, *119*, 337.
[10] S. Kumar, T. S. N. Sankara Narayanan, S. Ganesh Sundara Raman, S. K. Seshadri, *Corros. Sci.* **2010**, *52*, 711.
[11] M. Jamesh, S. Kumar, T. S. N. Sankara Narayanan, *J. Mater. Eng. Perform.* **2012**, *21*, 900.
[12] M. F. Lopez, J. A. Jimenez, A. Gutierrez, *Electrochim. Acta* **2003**, *48*, 1395.
[13] D. Velten, V. Biehl, F. Aubertin, B. Valeske, W. Possart, J. Breme, *J. Biomed. Mater. Res.* **2002**, *59*, 18.
[14] M. L. Escudero, J. L. Gonzalez-Carrasco, C. Garcia-Alonso, E. Ramirez, *Biomaterials* **1995**, *16*, 735.
[15] D. Siva Rama Krishna, Y. L. Brama, Y. Sun, *Tribol. Int.* **2007**, *40*, 329.
[16] A. Bloyce, P. Y. Qi, H. Dong, T. Bell, *Surf. Coat. Technol.* **1998**, *107*, 125.
[17] Q. Mohsen, S. A. Fadl-Allah, *Mater. Corros.* **2011**, *62*, 310.
[18] M. Jamesh, S. Kumar, T. S. N. Sankara Narayanan, *Corros. Sci.* **2011**, *53*, 645.
[19] H. Guleryuz, H. Cimenoglu, *Biomaterials* **2004**, *25*, 3325.
[20] H. Guleryuz, H. Cimenoglu, *Surf. Coat. Technol.* **2005**, *192*, 164.
[21] W. Yan, X. X. Wang, *J. Mater. Sci.* **2004**, *39*, 5583.
[22] A. R. Ebrahimi, F. Zarei, R. A. Khosroshahi, *Surf. Coat. Technol.* **2008**, *203*, 199.
[23] M. C. Garcia-Alonso, L. Saldana, G. Valles, J. L. Gonzalez-Garrasco, J. Gonzalez-Cabrero, M. E. Martinez, E. Gil-Garay, L. Munuera, *Biomaterials* **2003**, *24*, 19.
[24] H. L. Du, P. K. Datta, D. B. Lewis, J. S. Burnell-Gray, *Corros. Sci.* **1994**, *36*, 631.
[25] K. Nakajima, K. Terao, T. Miata, *Mater. Sci. Eng. A* **1998**, *243*, 176.
[26] J. A. Hall, *Int. J. Fatigue* **1997**, *19*, 23.
[27] C. Leinenbach, D. Eifler, *Acta Biomater.* **2009**, *5*, 2810.
[28] M. Javidi, M. E. Bahrololoom, S. Javadpour, J. Ma, *Mater. Corros.* **2009**, *60*, 336.
[29] A. S. Mogoda, Y. H. Ahmad, W. A. Badawy, *J. Appl. Electrochem.* **2004**, *34*, 873.
[30] A. Robin, I. I. Rosa, H. R. Z. Sandim, *J. Appl. Electrochem.* **2001**, *31*, 455.
[31] E. Mccafferty, *Introduction to Corrosion Science*, Springer, New York **2010**, 212.
[32] E. Klar, P. K. Samal, *Powder Metallurgy Stainless Steels: Processing, Microstructures, and Properties*, ASM International, Materials Park, OH **2007**, 155.
[33] D. Marecil, D. Sutiman, A. Cailean, I. Cretescu, *Environ. Eng. Manage. J.* **2008**, *7*, 701.
[34] G. S. Firstov, R. G. Vitchev, H. Kumar, B. Blanpain, J. Van Humbeeck, *Biomaterials* **2002**, *23*, 4863.
[35] S. Barisona, S. Cattarina, S. Daolioa, M. Musiania, A. Tuissib, *Electrochim. Acta*, **2004**, *50*, 11.

(Received: August 14, 2011) W6321
(Accepted: May 19, 2012)